CBMeMBer Filter based Resolvable Group Target Tracking via Graph Theory and Leader-Follower Model

Xinchao Zhu[1], Chaoqun Yang[2], Chengwei Zhou[1,3], and Zhiguo Shi[1,4]

[1] College of Information Science and Electronic Engineering, Zhejiang University, Hangzhou 310027, China
[2] School of Automation, Southeast University, Nanjing 210092, China
[3] Jinhua Institute of Zhejiang University, Jinhua 321037, China
[4] International Joint Innovation Center, Zhejiang University, Haining 314400, China
E-mail: xincz@zju.edu.cn, ycq@seu.edu.cn, zhouchw@zju.edu.cn, shizg@zju.edu.cn

***Abstract*—Resolvable group target tracking is of great challenge due to the complex motion interaction between group targets, which leads to tracking performance degradation. To solve this problem, a cardinality-balanced multi-target multi-Bernoulli filter based on the graph theory and leader-follower model is proposed. In the proposed filter, firstly, the group targets are divided into leaders and followers by mean of the leader-follower model. Furthermore, the graph theory is used to establish the state transition equations between those divided group targets. Lastly, the process of state prediction is given, and its corresponding implementation is derived by Gaussian mixture approximations. Simulation experiments verify the superiority and effectiveness of the proposed filter.**

***Index Terms*—Graph theory, leader-follower model, multi-target multi-Bernoulli filter, resolvable group target tracking.**

I. Introduction

Resolvable group target tracking (RGTT) has been intensively studied in the field of radar, sonar, visual and so on. [1]–[5]. Resolvable group target is defined as a group of targets that interact with the motion model, and each target locates in a single resolution cell [6]. In such scenario, different from the traditional multi-target tracking, the interaction between group targets plays an indispensable role in the tracking or filtering process [7]–[9]. Therefore, how to design the interaction model between group targets is critical for group target tracking, which can further improve tracking performance [10].

Along this direction, there are diverse interaction models for group target tracking, which can be classified into different categories depending on the motion state of group targets. Specifically, the existing interaction methods for RGTT can be mainly classified into two categories, i.e., stochastic differential equation (SDE) and graph structure. For the SDE methods, [11] adopts SDE to describe the repulsive force and restoring force between group targets in order to establish a group target motion model. To further improve the tracking performance, [12] utilizes the SDE to derive a single-target state transition equation (STE) for revising the prediction process of the standard multi-Bernoulli filter. For the graph structure methods, they regard targets as vertices and the relationships between targets as lines in the graph, such that the topological structure between group targets can be formulated based on the graph theory [13]. For example, [14] relies on the graph structure methods to represent the interaction between groups and then obtain an identification method of the group splitting and merging. [15] combines the SDE and graph theory to obtain the labeled multi-Bernoulli (LMB) filter for tracking group targets with interaction.

After determining the group targets interaction model, the choice of filtering methods is also crucial. Due to the excessive number of group targets, it will lead to complex calculation problems in the data association process [16]–[18]. Compared with traditional data association methods, such as joint probabilistic data association filter (JPDAF) [19] and multiple hypothesis tracker (MHT) [20], random finite set (RFS) based filters provide a more effective solution as it does not require data association [21], [22]. For example, probability hypothesis density (PHD) filter [23] can propagate the first-order moment of multi-target states to complete the prediction, whereas cardinalized PHD (CPHD) filter [24] propagates the moments and cardinality distributions to implement target tracking. Different from PHD and CPHD filters, multi-Bernoulli (MB) filter propagates the parameters of a MB distribution to approximate the posterior multi-target density. To further alleviate estimation error in the MB filter, the cardinality balanced multi-target multi-Bernoulli filter (CBMeMBer) filter is proposed in [25]. Unfortunately, the trajectories of targets cannot be obtained in the above-mentioned filters. To solve this dilemma, the generalized labeled multi-Bernoulli (GLMB) [26] and labeled multi-Bernoulli (LMB) [27] filter are proposed to output complete trajectories. Moreover, there are close link between traditional filters and some RFS filters when targets can be born with large spatial uncertainties [28].

This work was partially supported by National Natural Science Foundation of China (U21A20456, 62303109), Fundamental Research Funds for the Central Universities (226-2023-00111, 226-2024-00004), Zhishan Young Scholar Research Fund of Southeast University (2242024RCB0011), and Zhejiang University Education Foundation Qizhen Scholar Foundation.

In general, the selection of filters is flexible, and can be changed according to the practical scenarios [29], [30].

Although most of the above-mentioned filters exhibit excellent performance in the specific scenarios, it is worth noting that most of the existing works still face serious challenges in the RGTT scenario, such as the limitations of target interaction models and the accuracy of group targets tracking, etc. Thus, in this paper, we propose a novel CBMeMBer filter based on graph theory and leader-follower model, namely, GTLF-CBMeMBer filter, which is shown in Fig. 1. Firstly, it utilizes the leader-follower model to divide group targets. Secondly, the graph theory is adopted to establish the STE of leader and follower. Finally, we derive the prediction step and its corresponding implementation to obtain the complete filter for the resolvable group target tracking scenario.

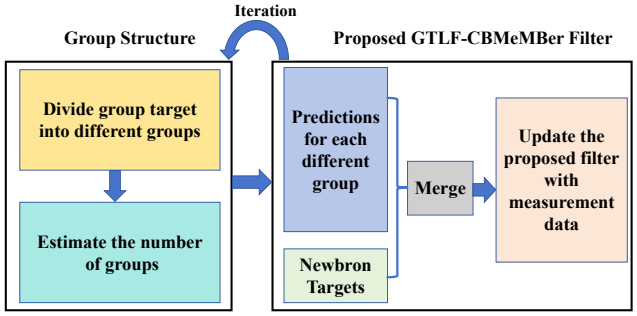

Fig. 1. The structure of proposed GTLF-CBMeMBer filter.

In summary, the main contributions of this paper are as follows.

1) By using the leader-follower model, the group structure estimation and separation method is proposed, and then, the STE for group targets is formulated based on the graph theory. Different from the graph structure method in [14], we consider the target position and velocity simultaneously for a given group to ensure a higher accuracy of motion model.

2) We propose the GTLF-CBMeMBer filter and deduce its prediction along with the corresponding implementation methods. Simulation verifies that the proposed filter is superior to the traditional CBMeMBer filter.

The remainder of this paper is organized as follows. Section II introduces the standard CBMeMBer filter, graph theory and leader-follower model. Sections III derives the STE of group target. The prediction of GTLF-CBMeMBer filter and its implementation are given in Section IV. Finally, conclusions are drawn in Section V.

II. PRELIMINARIES

This section provides the basic concepts of the standard CBMeMBer filter, graph theory, and the leader-follower model.

A. Standard CBMeMBer Filter

1) Bernoulli RFS and Multi-Bernoulli RFS: A Bernoulli RFS on state space $\mathbb{X}$ can be treated as the existence probability r and a state density $p(x)$, and its probability density is

$$\pi(X) = \begin{cases} 1-r, & X = \emptyset \\ r \cdot p(x), & X = \{x\}. \end{cases} \tag{1}$$

Similarly, a multi-Bernoulli (MB) RFS is a union of a fixed number of independent Bernoulli RFSs $X^{(i)}$ with the existence probability of the i-th target $r^{(i)} \in [0,1]$ and the probability density of the state conditioned on its existence $p^{(i)}(x)$, $i = 1, ..., M$, i.e., $X = \cup_{i=1}^{M} X^{(i)}$. Hence, the MB RFS is completely characterized by MB parameter set $\{(r^{(i)}, p^{(i)})\}_{i=1}^{M}$. For $\{x_1, x_2, \cdots, x_n\}$ in X, the probability distribution can be expressed as $\pi(\emptyset) = \prod_{j=1}^{M}(1 - r^{(j)})$ and

$$\pi(\{x_1, \ldots, x_n\}) = \pi(\emptyset) \sum_{1 \le i_1 \ne \cdots \ne i_n \le M} \prod_{j=1}^{n} \frac{r^{(i_j)} p^{(i_j)}(x_j)}{1 - r^{(i_j)}}. \tag{2}$$

2) Prediction and Update Step: The standard CBMeMBer filter is mainly composed of prediction and update steps. For the step of prediction, at time $k-1$, suppose that the posterior multi-target density is a multi-Bernoulli distribution given by

$$\pi_{k-1} = \{(r_{k-1}^{(i)}, p_{k-1}^{(i)})\}_{i=1}^{M_{k-1}}, \tag{3}$$

then the predicted multi-target density is also a multi-Bernoulli distribution and is given by

$$\pi_{k|k-1} = \{(r_{P,k|k-1}^{(i)}, p_{P,k|k-1}^{(i)})\}_{i=1}^{M_{k-1}} \cup \{(r_{\Gamma,k}^{(i)}, p_{\Gamma,k}^{(i)})\}_{i=1}^{M_{\Gamma,k}}, \tag{4}$$

where

$$r_{P,k|k-1}^{(i)} = r_{k-1}^{(i)} \langle p_{k-1}^{(i)}, P_{s,k} \rangle, \tag{5}$$

$$p_{P,k|k-1}^{(i)}(x) = \frac{\langle f_{k-1}(x\,|\cdot), p_{k-1}^{(i)} P_{s,k} \rangle}{\langle p_{k-1}^{(i)}, P_{s,k} \rangle}. \tag{6}$$

Here, $f_{k-1}(\cdot\,|\varsigma)$ denotes the single target transition density at time k, given previous state ς, whereas $P_{s,k}(\varsigma)$ is the probability of target existence at time k, given previous state ς. $\langle f, g \rangle = \int f(x)g(x)dx$, and $\{r_{\Gamma,k}^{(i)}, p_{\Gamma,k}^{(i)}\}_{i=1}^{M_{\Gamma,k}}$ denotes birth parameter of the multi-Bernoulli RFS at time k.

For the step of update, at time k, suppose that the predicted multi-target density is a multi-Bernoulli distribution in the form of

$$\pi_{k|k-1} = \{(r_{k|k-1}^{(i)}, p_{k|k-1}^{(i)})\}_{i=1}^{M_{k|k-1}}. \tag{7}$$

Then, a multi-Bernoulli approximation with cardinality-unbiased can be used to model the posterior multi-target density, i.e.,

$$\pi_k \approx \{(r_{L,k}^{(i)}, p_{L,k}^{(i)})\}_{i=1}^{M_{k|k-1}} \cup \{(r_{U,k}^{*}(z), p_{U,k}^{*}(\cdot; z))\}_{z \in Z_k}, \tag{8}$$

where

$$r_{L,k}^{(i)} = r_{k|k-1}^{(i)} \frac{1 - \langle p_{k|k-1}^{(i)}, P_{D,k} \rangle}{1 - r_{k|k-1}^{(i)} \langle p_{k|k-1}^{(i)}, P_{D,k} \rangle}, \tag{9}$$

$$p_{L,k}^{(i)}(x) = p_{k|k-1}^{(i)}(x) \frac{1 - P_{D,k}}{1 - \langle p_{k|k-1}^{(i)}, P_{D,k} \rangle}, \tag{10}$$

$$r^*_{U,k}(z)=\frac{\sum_{i=1}^{M_{k|k-1}}\frac{r^{(i)}_{k|k-1}(1-r^{(i)}_{k|k-1})\langle p^{(i)}_{k|k-1},\psi_{k,z}\rangle}{(1-r^{(i)}_{k|k-1}\langle p^{(i)}_{k|k-1},P_{D,k}\rangle)^2}}{\kappa_k(z)+\sum_{i=1}^{M_{k|k-1}}\frac{r^{(i)}_{k|k-1}\langle p^{(i)}_{k|k-1},\psi_{k,z}\rangle}{1-r^{(i)}_{k|k-1}\langle p^{(i)}_{k|k-1},P_{D,k}\rangle}}, \tag{11}$$

$$p^*_{U,k}(x;z)=\frac{\sum_{i=1}^{M_{k|k-1}}\frac{r^{(i)}_{k|k-1}}{1-r^{(i)}_{k|k-1}}p^{(i)}_{k|k-1}(x)\psi_{k,z}(x)}{\sum_{i=1}^{M_{k|k-1}}\frac{r^{(i)}_{k|k-1}}{1-r^{(i)}_{k|k-1}}\langle p^{(i)}_{k|k-1},\psi_{k,z}\rangle}. \tag{12}$$

Here, Z_k is the measurement set at time k. $\psi_{k,z}(x)=g_k(z\,|x\,)P_{D,k}(x)$, where $g_k(\cdot\,|x\,)$ and $P_{D,k}(x)$ respectively denote the single target measurement likelihood and probability of target detection at time k, given current state x. $\kappa_k(\cdot)$ is the intensity of Poisson clutter.

B. Graph Theory

Graph theory provides an effective system modeling method for group target movement. A graph G is a pair (ν,ε) that consists of a set of vertices $\nu=\{1,2,...,n\}$ and edge $\varepsilon\subseteq\{(i,j):i,j\in\nu,j\neq i\}$, which means that the graph is in general directed and has no self-loops. Whether $(i,j)\in\varepsilon\Leftrightarrow(j,i)\in\varepsilon$ is established, the graph can be defined as undirected and directed graph, respectively.

The adjacency matrix $\boldsymbol{A}$ of a graph is a nonzero elements matrix, and it satisfies $a_{i,j}\in\boldsymbol{A}\neq 0\Leftrightarrow(j,i)\in\varepsilon$ and $\boldsymbol{A}^{\mathrm{T}}=\boldsymbol{A}$. For an undirected graph, the set of neighbors of node is defined as

$$M_i=\{j\in\nu:a_{i,j}\neq 0\}=\{j\in\nu:(i,j)\in\varepsilon\}. \tag{13}$$

C. Leader-Follower (LF) Model

Different from the traditional target motion model where all targets are moving independently, the targets in the LF model have two target motion states.

- Target being a leader (TL) determines the primary motion state of the group.
- Target being a follower (TF) is guided by the TL within the same group, and its motion state is constrained by both itself and the TL.

In a RGTT scenario, it consists of different group target interaction, including group merging and splitting. As shown in Fig. 2, the TL is responsible for interacting with the TF, whereas the TF is only responsible for interacting with the TL to make corresponding adjustments according to the TL.

III. The STE For Group Target

Different from traditional multi-target tracking scenarios, group target tracking pays more attention to the estimation of group state, structure, and number of subgroups. In this section, we derive the STE of group target to enhance the prediction process of the standard CBMeMBer filter and present the graph structure method to estimate the number of subgroups.

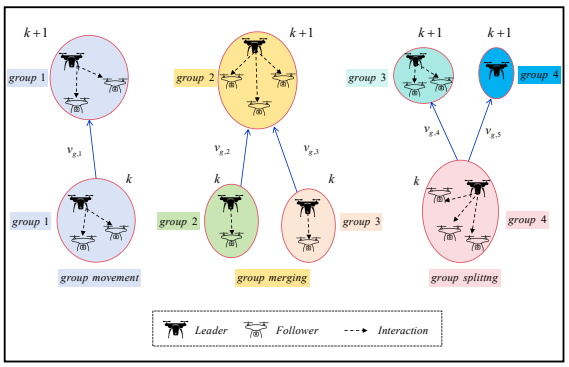

Fig. 2. The schematic diagram of the LF model in a RGTT scenario.

A. Dynamic Models for TL

Before specifying the motion state for the TL, two necessary assumptions are indicated as follows.

Assumption 1. *Each group can only contain at most one leader.*

Assumption 2. *The foremost target in the movement direction is the leader in each group.*

For the TL, its motion state is only related to itself preceding motion state, so it can be modeled using a general movement model. For TL j with the state $\mathbf{x}^{(j)}_k=[x^{(j)}_k,v^{(j)}_{x,k},y^{(j)}_k,v^{(j)}_{y,k}]^\top$, where the superscript $\top$ denotes matrix transpose, the movement state model of leader can be expressed as

$$\begin{aligned}\mathbf{x}^{(j)}_{k+1}&=\mathbf{F}^{(j)}_k\mathbf{x}^{(j)}_k+\mathbf{v}^{(j)}_k,\\ \mathbf{z}^{(j)}_{k+1}&=\mathbf{H}^{(j)}_k\mathbf{x}^{(j)}_k+\mathbf{n}^{(j)}_k,\end{aligned} \tag{14}$$

where $\mathbf{F}^{(j)}_k$ is the state transition matrix, and $\mathbf{H}^{(j)}_k$ is the measurement matrix. Here, $\mathbf{v}^{(j)}_k$ and $\mathbf{n}^{(j)}_k$ are zero-mean Gaussian noise that are independent of each other, and the corresponding covariance is recorded as $\mathbf{Q}^{(j)}_k$ and $\mathbf{R}^{(j)}_k$, respectively. Then, the state transition density and likelihood function can be expressed as

$$f\left(\mathbf{x}^{(j)}_{k+1}\middle|\mathbf{x}^{(j)}_k\right)=\mathcal{N}(\mathbf{x}^{(j)}_k;\mathbf{F}^{(j)}_k\mathbf{x}^{(j)}_k,\mathbf{Q}^{(j)}_k), \tag{15}$$

$$g\left(\mathbf{z}^{(j)}_{k+1}\middle|\mathbf{X}^{(j)}_{k+1}\right)=\mathcal{N}(\mathbf{z}^{(j)}_k;\mathbf{H}^{(j)}_k\mathbf{x}^{(j)}_{k+1},\mathbf{R}^{(j)}_{k+1}), \tag{16}$$

where $\mathcal{N}(\cdot;\boldsymbol{m},\boldsymbol{P})$ is the Gaussian density with mean $\boldsymbol{m}$ and covariance $\boldsymbol{P}$.

B. Dynamic Model for TF

For TF i with the state $\mathbf{x}^{(i)}_k=[x^{(i)}_k,v^{(i)}_{x,k},y^{(i)}_k,v^{(i)}_{y,k}]^\top$ in which $i\neq j$, its state is mainly dependent on TL j. Then, the state of TF i can be modeled via the graph theory

$$\begin{aligned}a_i&=\alpha(x^{(i)}_k-x^{(j)}_k),\\ b_i&=\beta(v^i_{x,k}-v^j_{x,k}),\\ c_i&=\alpha(y^{(i)}_k-y^{(j)}_k),\\ d_i&=\beta(v^{(i)}_{y,k}-v^{(j)}_{y,k}),\end{aligned} \tag{17}$$

where α and β are the position and velocity effects of the TL on TF, respectively. The larger the value of α, the faster the TF will approach the TL, and their relative positions will become smaller.

Consider the following linear model for TF $\mathbf{x}_k^{(i)}$ in group G_i with directed graph structure

$$\mathbf{x}_{k+1}^{(i)} = \sum_{l\in g(i)} \omega_{k-1}^{(i)}(l)\left[\mathbf{F}_k^{(i)}\mathbf{x}_k^{(j)} + \Delta\mathbf{b}_k^{(i)}\right] + \mathbf{v}_k^{(i)}, \tag{18}$$

where $g(i)$ is a vertex set denoting all the father vertices for vertex i, and

$$\mathbf{F}_k^{(i)} = \begin{bmatrix} 1 & T & 0 & 0 \\ 0 & 1 & 0 & 0 \\ 0 & 0 & 1 & T \\ 0 & 0 & 0 & 1 \end{bmatrix}, \tag{19}$$

$$\Delta\mathbf{b}_k^{(i)} = \left[\frac{b_i}{\beta}T + \frac{a_i}{\alpha}, \frac{b_i}{\beta}, \frac{d_i}{\beta}T + \frac{c_i}{\alpha}, \frac{d_i}{\beta}\right]^\top, \tag{20}$$

$$\sum_{l\in g(i)} \omega_{k-1}^{(i)}(l) = 1, \quad \omega_{k-1}^{(i)}(l) \in [0,1]. \tag{21}$$

To formulate the interaction process of dynamic model between TL and TF, a real distance variable $\Delta\mathbf{d}_k^{(i)}$ is introduced to establish the connections between them. Different from $\Delta\mathbf{b}_k^{(i)}$, the real distance variable $\Delta\mathbf{d}_k^{(i)}$ at time k can be obtain as

$$\mathbf{x}_k^{(i)} = \mathbf{x}_k^{(j)} + \Delta\mathbf{d}_k^{(i)}. \tag{22}$$

Combining (18) and (22), based on the **Assumption 1**, we have $g(i) = 1$, and $\mathbf{x}_{k+1}^{(i)}$ can be simplified as

$$\begin{aligned} \mathbf{x}_{k+1}^{(i)} &= \mathbf{F}_k^{(i)}\mathbf{x}_k^{(i)} - \mathbf{F}_k^{(i)}\Delta\mathbf{d}_k^{(i)} + \Delta\mathbf{b}_k^{(i)} + \mathbf{v}_k \\ &= \mathbf{F}_k^{(i)}\mathbf{x}_k^{(i)} + \Delta\mathbf{B}_{\mathrm{k}} + \mathbf{v}_k \\ &= \mathbf{F}_k^{(i)}\mathbf{x}_k^{(i)} + \mathbf{V}_{k,0}, \end{aligned} \tag{23}$$

$$\Delta\mathbf{B}_{\mathrm{k}} = \Delta\mathbf{b}_k^{(i)} - \mathbf{F}_k^{(i)}\Delta\mathbf{d}_k^{(i)}, \quad \mathbf{V}_{k,0} = \Delta\mathbf{B}_{\mathrm{k}} + \mathbf{v}_k. \tag{24}$$

Proposition 1. *Given the dynamic model (18), if (1) The group target state model is one of the following models, such as the constant acceleration (CA), the constant velocity (CV) and the constant turn rate (CT) models; (2) The real distance variable is non-random, i.e., $E(\Delta\boldsymbol{d}_k^{(i)}) = \Delta\boldsymbol{b}_k^{(i)}$, where $E(\cdot)$ denotes the mathematical expectation. Then, the collaborative noise $\boldsymbol{v}_{k,0}$ is also Gaussian and can be expressed as*

$$\mathbf{V}_{k,0} \sim \mathcal{N}(0, \boldsymbol{N}_{k,0}), \tag{25}$$

$$\boldsymbol{N}_{k,0} = \mathbf{F}_k(\boldsymbol{P}_k^j - \boldsymbol{P}_k^i)\mathbf{F}_k^\top + \mathbf{Q}_k^{(i)}, \tag{26}$$

where $\mathbf{P}_k^j$ and $\mathbf{P}_k^i$ denotes the covariance of TL j and TF i, respectively. When $\mathbf{P}_k^j = \mathbf{P}_k^i$, the dynamic model of the TF will degenerate to the general multi-target tracking model, which means that the standard CBMeMBer filter can be directly used for group targets.

Proof: For the fixed formation and nonrandom displacement vector, the real distance variable $\Delta\mathbf{d}_k^{(i)}$ has the following forms

$$\Delta\mathbf{d}_k^{(i)} = [\Delta\mathbf{b}_{k,x}^{(i)}, 0, \Delta\mathbf{b}_{k,y}^{(i)}, 0]_{CV}, \tag{27}$$

$$\Delta\mathbf{d}_k^{(i)} = [\Delta\mathbf{b}_{k,x}^{(i)}, 0, 0, \Delta\mathbf{b}_{k,y}^{(i)}, 0, 0]_{CA,CT}. \tag{28}$$

where the subscript CV, CA and CT represent the corresponding motion model. Based on (23) and (27), it follows that the displacement is constant and equals to the true value, i.e., $E(\Delta\mathbf{d}_k^{(i)}) = \Delta\mathbf{b}_k^{(i)}$, so we have

$$E[\Delta\mathbf{B}_k] = \Delta\mathbf{b}_k^{(i)} - \mathbf{F}_k\Delta\mathbf{b}_k^{(i)} = (\mathbf{I} - \mathbf{F}_k)\Delta\mathbf{b}_k^{(i)} = 0. \tag{29}$$

Thus, the expectation of collaboration noise $\mathbf{V}_{k,0}$ and process noise $\mathbf{v}_k$ is equivalent, i.e., $E(\mathbf{V}_{k,0}) = E(\mathbf{v}_k)$, which means that the predicted states of group target tracking are equivalent to the general multi-target tracking.

Then, the state covariances can be obtained by

$$\begin{aligned} \Delta\boldsymbol{P}_{k+1|k} &= \mathbf{F}_k\boldsymbol{P}_k^{(j)}\mathbf{F}_k^\top + \mathbf{Q}_k - (\mathbf{F}_k\boldsymbol{P}_k^{(i)}\mathbf{F}_k^\top + \mathbf{Q}_k) \\ &= \mathbf{F}_k(\boldsymbol{P}_k^{(j)} - \boldsymbol{P}_k^{(i)})\mathbf{F}_k^\top. \end{aligned} \tag{30}$$

If $\boldsymbol{P}_k^{(j)} = \boldsymbol{P}_k^{(i)}$, we then have $\Delta\boldsymbol{P}_{k+1|k} = 0$, indicating that group target tracking is degenerates to the traditional multi-target tracking. ■

C. Structure Models for Group Targets

In general, the estimation of group targets can be classified into two steps, namely, target state estimation and group structure estimation. After obtaining the location information of the group targets, the group structure model for the group targets can be represented by the adjacency matrix.

Suppose that the target state set at time k is $\mathbf{X}_k = \{x_{k,1}, x_{k,2}, \cdots, x_{k,N(k)}\}$, the dependent relation of group targets is modeled by the adjacency matrix $\boldsymbol{A}_k$. Unfortunately, the connection relation cannot be directly derived because of the lack of prior information about the group structure, and thus, the deviation matrix $\boldsymbol{S}_k$ is used to estimate it. In particular, if the distance between two vertices is less than a threshold, they are considered to be related.

The deviation matrix can be defined by the distance between all pairs of vertices

$$\boldsymbol{S}_k = \begin{bmatrix} 0 & s_k(1,2) & \cdots & s_k(1,N(k)) \\ s_k(2,1) & 0 & \cdots & s_k(2,N(k)) \\ \vdots & \vdots & \ddots & \vdots \\ s_k(N(k),1) & s_k(N(k),2) & \cdots & 0 \end{bmatrix}, \tag{31}$$

where $s_k(i,j)$ is computed by ℓ_2-norm, i.e.,

$$s_k(i,j) = \|x_{k,i} - x_{k,j}\|_2. \tag{32}$$

Obviously, the deviation matrix is symmetric, i.e., $s_k(i,j) = s_k(j,i)$. Then, the adjacency matrix $\boldsymbol{A}_k$ can be given as

$$\boldsymbol{A}_k(i,j) = \begin{cases} 1, & s_k(i,j) < \tau \\ 0, & \text{otherwise} \end{cases} \tag{33}$$

where τ is a given distance threshold. After obtaining the adjacency matrix, the degree matrix $\boldsymbol{D}_k$ can be expressed as

$$\boldsymbol{D}_k = diag([d_{k,1}, d_{k,2}, \cdots, d_{k,N(k)}]), \tag{34}$$

where $diag([\cdot])$ stands for the diagonal matrix with

$$d_{k,i} = \sum\nolimits_{j=1}^{N(k)} \boldsymbol{A}_k(i,j). \tag{35}$$

Then, the Laplace matrix $\boldsymbol{L}_k$ can be expressed by $\boldsymbol{A}_k$ and $\boldsymbol{D}_k$ as

$$\boldsymbol{L}_k = \boldsymbol{D}_k - \boldsymbol{A}_k. \tag{36}$$

Based on the following *Lemma 1*, the number of groups can be obtained by the number of eigenvalues of 0 in the Laplace matrix $\boldsymbol{L}_k$.

Lemma 1. *The number of eigenvalues of* 0 *in the Laplacian matrix equals to the number of connected components in the graph [31].*

For example, suppose that the eigenvalues of the Laplace matrix $\boldsymbol{L}_k$ are $\{\lambda_{k,1}, \lambda_{k,2}, \cdots, \lambda_{k,N(k)}\}$, if the graph is connected, $\underbrace{\lambda_{k,j} = \cdots = \lambda_{k,j+n}}_{n} = 0$ and the other eigenvalues are non-zero, then the graph has $n+1$ exactly connected components.

IV. The proposed GTLF-CBMEMBER Filter

In group target tracking, it is crucial to establish an accurate interaction model for the group targets, which can further improve the tracking performance. Therefore, we first establish the STE of the group target and introduce it to the CBMeMBer filter framework. Then, the GTLF-CBMeMBer filter is proposed to improve the tracking accuracy in the group target tracking scenarios. Before elaborating the proposed filter, it is worth to emphasize that we only focus on the effect of group structure during the prediction step, while the update step still follows the standard CBMeMBer filter. In this section, the prediction step of the GTLF-CBMeMBer filter and the corresponding Gaussian mixture (GM) implementation will be presented.

A. Prediction Step

Suppose that the motions of different groups are mutually independent, then the prediction process can be implemented in parallel. Given the current MB density with $\{(r_k^{(i)}, p_k^{(i)})\}_{i=1}^{M_{k,g}}$ and the cardinality of groups G, the MB density of groups at time k can be obtained by

$$\pi_k = \cup_{g=1}^{G} \{(r_{k,g}^{(i)}, p_{k,g}^{(i)})\}_{i=1}^{M_{k,g}}. \tag{37}$$

Furthermore, assuming that target i is the follower and j is the leader, for the g-th groups, the predicted MB density can be denoted as

$$\begin{aligned}\pi_k = \cup_{g=1}^{G} &\underbrace{\{(r_{P,k,g}^{(i)}, p_{P,k,g}^{(i)})\}_{i=1}^{M_{k,g}}}_{Follower} \cup \underbrace{\{(r_{P,k,g}^{(j)}, p_{P,k,g}^{(j)})\}_{j\neq i}}_{Leader} \\ &\cup \underbrace{\{(r_{\Gamma,k}^{(m)}, p_{\Gamma,k}^{(m)})\}_{m=1}^{M_{\Gamma,k}}}_{Newbron}\end{aligned} \tag{38}$$

where

$$r_{P,k,g}^{(i)} = r_{k-1,g}^{(i)} \langle p_{k-1,g}^{(i)}, P_{s,k}^{(i)} \rangle, \tag{39}$$

$$p_{p,k,g}^{(i)} = \frac{\langle f_{k-1}^{(i)}(x\,|\cdot), p_{k-1,g}^{(i)} P_{s,k} \rangle}{\langle p_{k-1,g}^{(i)}, P_{s,k} \rangle}, \tag{40}$$

and

$$r_{P,k,g}^{(j)} = r_{k-1}^{(j)} \langle p_{k-1,g}^{(j)}, P_{s,k}^{(j)} \rangle, \tag{41}$$

$$p_{p,k,g}^{(j)} = \frac{\langle f_{k-1}^{(j)}(x\,|\cdot), p_{k-1,g}^{(j)} P_{s,k} \rangle}{\langle p_{k-1,g}^{(j)}, P_{s,k} \rangle}. \tag{42}$$

Here, $f_{k-1}^{(i)}(x\,|\cdot)$ and $f_{k-1}^{(j)}(x\,|\cdot)$ are the STEs of TF i and TL j, respectively.

B. GM-based Implementation of the Prediction Step

In this section, GM approximations [30] are adopted as the implementation tool. Specifically, target m in the g-th group can be expressed as

$$P_{k,g}^{(m)}(\mathbf{x}) = \sum_{q=1}^{J_{k,g}^{(m)}} \omega_{k,g}^{(m,q)} \mathcal{N}(\mathbf{x}; \mathbf{x}_{k,g}^{(m,q)}, \boldsymbol{P}_{k,g}^{(m,q)}), \tag{43}$$

where $J_{k,g}^{(m)}$ denotes the number of Gaussian components (GCs), $\omega_{k,g}^{(m,q)}$ is the weight, $\mathbf{x}_{k,g}^{(m,q)}$ and $\boldsymbol{P}_{k,g}^{(m,q)}$ are the mean and covariance of the q-th Gaussian component, respectively.

On one hand, based on the prediction process (38)-(42) and GM approximations, the prediction step of TF i in the g-th group is given by

$$r_{P,k,g}^{(i)} = r_{k-1}^{(i)} P_{s,k}, \tag{44}$$

$$P_{k,g}^{(i)}(\mathbf{x}) = \sum_{q=1}^{J_{k,g}^{(i)}} \hat{\omega}_{k,g}^{(i,q)} \mathcal{N}(\mathbf{x}; \hat{\mathbf{x}}_{k,g}^{(i,q)}, \hat{\boldsymbol{P}}_{k,g}^{(i,q)}), \tag{45}$$

where

$$\begin{aligned}\hat{\omega}_{k,g}^{(i,q)} &= \omega_{k,g}^{(i,q)}, \\ \hat{\mathbf{x}}_{k,g}^{(i,q)} &= \mathbf{F}_{k-1}^{(i)} \mathbf{x}_{k-1,g}^{(i,q)} + \Delta \mathbf{B}_{k,g}^{(i)}, \\ \hat{\boldsymbol{P}}_{k,g}^{(i,q)} &= \mathbf{F}_{k-1,i} (\boldsymbol{P}_{k-1,g}^{(j,q)} - \boldsymbol{P}_{k-1,g}^{(i,q)}) \mathbf{F}_{k-1,i}^{\top} + \mathbf{R}_{k-1,g}^{(i)}.\end{aligned} \tag{46}$$

On the other hand, the prediction process of TL j in the g-th group is given by

$$r_{P,k,g}^{(j)} = r_{k-1}^{(j)} P_{s,k}, \tag{47}$$

$$P_{k,g}^{(j)}(\mathbf{x}) = \sum_{q=1}^{J_{k,g}^{(j)}} \hat{\omega}_{k,g}^{(j,q)} \mathcal{N}(\mathbf{x}; \hat{\mathbf{x}}_{k,g}^{(j,q)}, \hat{\boldsymbol{P}}_{k,g}^{(j,q)}), \tag{48}$$

where

$$\begin{aligned}\hat{\omega}_{k,g}^{(j,q)} &= \omega_{k,g}^{(j,q)}, \\ \hat{\mathbf{x}}_{k,g}^{(j,q)} &= \mathbf{F}_{k-1}^{(j)} \mathbf{x}_{k-1}^{(j)}, \\ \hat{\boldsymbol{P}}_{k,g}^{(j,q)} &= \mathbf{F}_{k-1,j} \boldsymbol{P}_{k-1,g}^{(j,q)} \mathbf{F}_{k-1,j}^{\top} + \mathbf{R}_{k-1,g}^{(j)}.\end{aligned} \tag{49}$$

TABLE I
NEWBORN TARGETS INFORMATION

Target ID	Init. Loc(m)	Init.Vel(m/s)	Brith/Death(s)
1	[100, 800]	[24.5, 0]	1/60
2	[100, 900]	[24.5, 0]	1/60
3	[200, 850]	[25, 0]	1/60
4	[500, 300]	[30, 2]	5/45
5	[500, 500]	[29.5, -2]	5/45
6	[350, 1500]	[30, 0]	10/55
7	[300, 1450]	[29.5, 0]	10/55
8	[300, 1400]	[29.5, 0]	10/55
9	[350, 1350]	[30, 0]	10/55
10	[1000, 600]	[-15, 15]	20/60
11	[950, 600]	[-15, 15]	20/60

According to (46) and (49), the predicted state of TF depends not only on the update state of TL, but also on its own last update state, whereas TL is only influenced by its own preceding movement state. Therefore, the structure of the group targets needs to be estimated before performing state prediction.

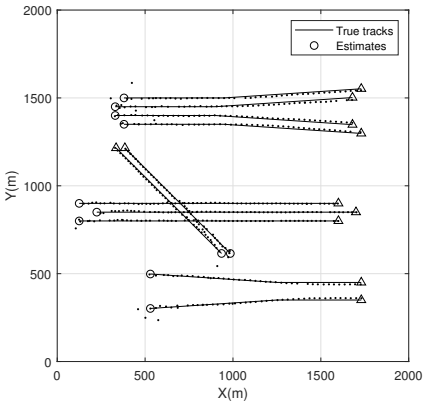

Fig. 3. Ground truth trajectories of the targets, where'◯/△' denotes the starting/ending point of one trajectory.

V. PERFORMANCE EVALUATION

In this section, simulation experiments are provided to evaluate the tracking performance of the proposed GTLF-CBMeMBer filter in terms of optimal sub-pattern assignment (OSPA) with Euclidean distance $p = 1$ and cutoff parameter $c = 100$ m. For both standard CBMeMBer filter and the proposed GTLF-CBMeMBer filters, the detection probability is P_d= 0.98, and the probability of survival is P_s= 0.99. The clutter density is uniform with 10 clutter points in average, the sampling period is $T = 1$s, $\alpha = 0.99$, $\beta = 0.985$, $\tau = 150$m. The birth is an MB RFS with the parameter $\pi_B = \{(r_{B,k}^{(i)}, p_{B,k}^{(i)})\}_{i=1}^{11}$, where $r_{B,k}^{(i)} = 0.03$ and $p_{B,k}^{(i)} = \mathcal{N}(x; x_B^{(i)}, P_B)$ with P_B = diag($[50^2, 30^2, 50^2, 30^2]$), and the standard deviation of the measurement noise covariance is

$$R = diag([\sigma_x^2, \sigma_y^2]^\top) \tag{50}$$

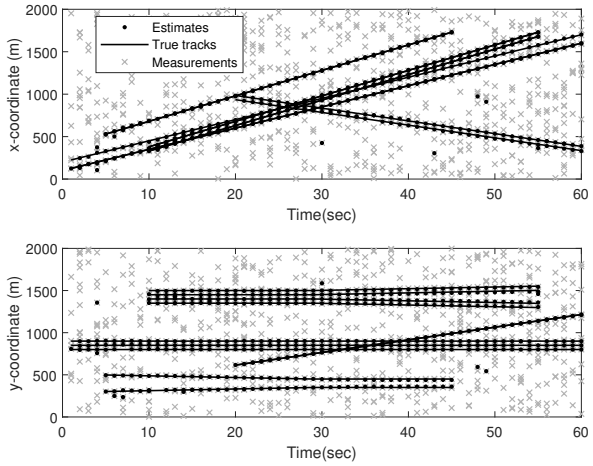

Fig. 4. The state estimation of the proposed filter.

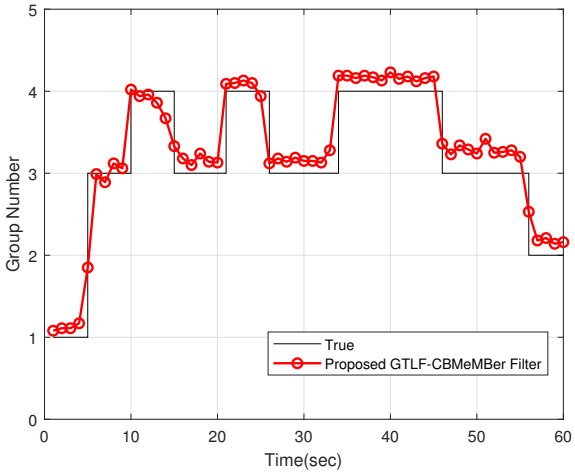

Fig. 5. The group number estimation result of the proposed filter.

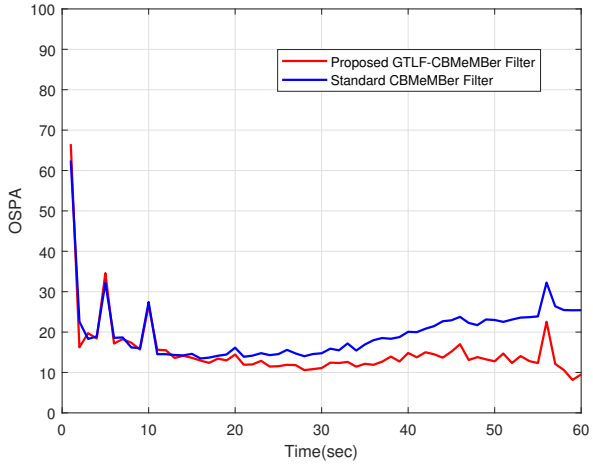

Fig. 6. The comparison of OSPA distance between the proposed GTLF-CBMeMBer filter and the standard CBMeMBer filter.

with $\sigma_x = 10$m and $\sigma_y = 5$m. Furthermore, all simulation results are averaged by 100 Monte Carlo (MC) trials.

Consider the scenario with four subgroup targets in the surveillance region [0,2000]×[0,2000] m^2, where the initial state and survival time are given in Table 1, and the target trajectories are shown in Fig. 3. We plot the x and y components (versus time) of the true trajectories, measurements, and GTLF-CBMeMBer filter estimates. Obviously, the proposed filter demonstrates a well-tracking performance and can accurately track all targets in the RGTT scenario.

Different from the standard CBMeMBer filter, the proposed filter is capable of estimating the number of groups. As shown in Fig. 5, when $T = 15s$, targets 10 and 11 merge into a single group, resulting in a decrease in the number of groups; when $T = 35s$, targets 6, 7, 8, and 9 split into two groups, resulting in an increase in the number of groups. It is obvious from Fig. 5 that the proposed GTLF-CBMeMBer filter accurately estimates the number of group targets. Note that, the standard CBMeMBer filter is not capable of estimating the number of groups due to the lack of prediction of group structure.

Then, the comparisons on average OSPA distance is given in Fig. 6. Due to the fact that the interaction model of group targets is accurately established in the step of target prediction, the proposed filter can accurately establish the interaction between group targets to improve prediction accuracy. It is depicted in Fig. 6 that the proposed GTLF-CBMeMBer filter exhibits a better performance than the standard CBMeMBer filter.

VI. Conclusion

In this paper, by means of the graph theory and leader-follower model, we proposed a GTLF-CBMeMBer filter for the resolvable group targets tracking scenario. First, we derived the STE of the TL and the TF based on graph theory, respectively. Then, combining the CBMeMBer filter for the STE, we derived the main steps of the proposed filter. Simulation results show that the proposed GTLF-CBMeMBer filter is superior to the standard CBMeMBer filter in terms of group target tracking accuracy.

References

[1] Z. Lu, W. Hu, Y. Liu, and T. Kirubarajan, "Seamless group target tracking using random finite sets," *Signal Process.*, vol. 176, Art. no. 107683, 2020.

[2] Z. Shi, X. Chang, C. Yang, Z. Wu, and J. Wu, "An acoustic-based surveillance system for amateur drones detection and localization," *IEEE Trans. Veh. Technol.*, vol. 69, no. 3, pp. 2731–2739, 2020.

[3] R. Mahler, *Statistical Multisource-Multitarget Information Fusion*. Artech, London, 2007.

[4] X. Zhu, L. Tu, S. Zhou, and Z. Zhang, "Robust variability index CFAR detector based on Bayesian interference control," *IEEE Transactions on Geoscience and Remote Sensing*, vol. 60, pp. 1–9, 2021.

[5] H. Zheng, C. Zhou, Z. Shi, Y. Gu, and Y. D. Zhang, "Coarray tensor direction-of-arrival estimation," *IEEE Trans. Signal Process.*, vol. 71, pp. 1128–1142, 2023.

[6] G. Li, G. Li, and Y. He, "Distributed multiple resolvable group targets tracking based on hypergraph matching," *IEEE Sens. J.*, vol. 23, no. 9, pp. 9669–9676, 2023.

[7] Q. Li, B. I. Ahmad, and S. J. Godsill, "Sequential dynamic leadership inference using Bayesian Monte Carlo methods," *IEEE Trans. Aerosp. Electron. Syst.*, vol. 57, no. 4, pp. 2039–2052, 2021.

[8] C. Zhou, Y. Gu, Z. Shi, and M. Haardt, "Structured Nyquist correlation reconstruction for DOA estimation with sparse arrays," *IEEE Trans. Signal Process.*, vol. 71, pp. 1849–1862, 2023.

[9] C. Shi, Z. Tang, L. Ding, and J. Yan, "Multidomain resource allocation for asynchronous target tracking in heterogeneous multiple radar networks with nonideal detection," *IEEE Trans. Aerosp. Electron. Syst.*, vol. 60, no. 2, pp. 2016–2033, 2024.

[10] X. Shi, C. Yang, W. Xie, C. Liang, Z. Shi, and J. Chen, "Anti-drone system with multiple surveillance technologies: Architecture, implementation, and challenges," *IEEE Commun. Mag.*, vol. 56, no. 4, pp. 68–74, 2018.

[11] S. K. Pang, J. Li, and S. J. Godsill, "Detection and tracking of coordinated groups," *IEEE Trans. Aerosp. Electron. Syst.*, vol. 47, no. 1, pp. 472–502, 2011.

[12] G. Li, G. Li, and Y. He, "Resolvable group target tracking via multi-Bernoulli filter and its application to sensor control scenario," *IEEE Trans. Signal Process.*, vol. 70, pp. 6286–6299, 2022.

[13] X. Zhang, H. Liu, F. Meng, and X. Shen, "Group target tracking via jointly optimizing group partition and association," *Automatica*, vol. 153, Art. no. 111013, 2023.

[14] W. Liu, S. Zhu, C. Wen, and Y. Yu, "Structure modeling and estimation of multiple resolvable group targets via graph theory and multi-Bernoulli filter," *Automatica*, vol. 89, pp. 274–289, 2018.

[15] L. Li, Q. Wu, B. Yang, S. Wei, and J. Wang, "Labeled multi-Bernoulli filter based group target tracking using SDE and graph theory," in *Proc. Int. Conf. Inf. Fusion*, Sun City, South Africa, Nov. 2021, pp. 1–8.

[16] H. G. Hoang, B. N. Vo, B. T. Vo, and R. Mahler, "The Cauchy–Schwarz divergence for Poisson point processes," *IEEE Trans. Inf. Theory*, vol. 61, no. 8, pp. 4475–4485, 2015.

[17] M. Beard, B. T. Vo, B. N. Vo, and S. Arulampalam, "Void probabilities and Cauchy–Schwarz divergence for generalized labeled multi-Bernoulli models," *IEEE Trans. Signal Process.*, vol. 65, no. 19, pp. 5047–5061, 2017.

[18] B. Ristic and B. N. Vo, "Sensor control for multi-object state-space estimation using random finite sets," *Automatica*, vol. 46, no. 11, pp. 1812–1818, 2010.

[19] L. Svensson, D. Svensson, M. Guerriero, and P. Willett, "Set JPDA filter for multitarget tracking," *IEEE Trans. Signal Process.*, vol. 59, no. 10, pp. 4677–4691, 2011.

[20] S. S. Blackman, "Multiple hypothesis tracking for multiple target tracking," *IEEE Trans. Aerosp. Electron. Syst.*, vol. 19, no. 1, pp. 5–18, 2004.

[21] C. Yang, X. Cao, L. He, and H. Zhang, "Distributed multiple attacks detection via consensus AA-GMPHD filter," *IEEE Trans. Syst. Man Cybern. Syst.*, vol. 53, no. 12, pp. 7526–7536, 2023.

[22] C. Yang, X. Cao, and Z. Shi, "Road-map aided Gaussian mixture labeled multi-Bernoulli filter for ground multi-target tracking," *IEEE Trans. Veh. Technol.*, vol. 72, no. 6, pp. 7137–7147, 2023.

[23] R. P. Mahler, "Multitarget Bayes filtering via first-order multitarget moments," *IEEE Trans. Aerosp. Electron. Syst.*, vol. 39, no. 4, pp. 1152–1178, 2003.

[24] R. Mahler, "PHD filters of higher order in target number," *IEEE Trans. Aerosp. Electron. Syst.*, vol. 43, no. 4, pp. 1523–1543, 2007.

[25] B. T. Vo, B. N. Vo, and A. Cantoni, "The cardinality balanced multi-target multi-Bernoulli filter and its implementations," *IEEE Trans. Signal Process.*, vol. 57, no. 2, pp. 409–423, 2008.

[26] B. T. Vo and B. N. Vo, "Labeled random finite sets and multi-object conjugate priors," *IEEE Trans. Signal Process.*, vol. 61, no. 13, pp. 3460–3475, 2013.

[27] B. N. Vo, B. T. Vo, and D. Phung, "Labeled random finite sets and the Bayes multi-target tracking filter," *IEEE Trans. Signal Process.*, vol. 62, no. 24, pp. 6554–6567, 2014.

[28] E. Brekke and M. Chitre, "Relationship between finite set statistics and the multiple hypothesis tracker," *IEEE Trans. Aerosp. Electron. Syst.*, vol. 54, no. 4, pp. 1902–1917, 2018.

[29] K. Granstrom and U. Orguner, "A PHD filter for tracking multiple extended targets using random matrices," *IEEE Trans. Signal Process.*, vol. 60, no. 11, pp. 5657–5671, 2012.

[30] B. N. Vo and W. K. Ma, "The Gaussian mixture probability hypothesis density filter," *IEEE Trans. Signal Process.*, vol. 54, no. 11, pp. 4091–4104, 2006.

[31] R. Merris, "Laplacian matrices of graphs: A survey," *Linear Algebra Appl.*, vol. 197, pp. 143–176, 1994.